A BRIEF HISTORY OF FAST NEUTRON TELETHERAPY PART II - ADOLESCENCE: EXPANSION OF TECHNOLOGY

M. F. Moyers[1,2,3]

[1]Shanghai Proton and Heavy Ion Center / Department of Medical Physics, Shanghai, China 201321
[2]Shanghai Key Laboratory of Radiation Oncology, Shanghai, China 201321
[3]Shanghai Engineering Research Center of Proton and Heavy Ion Radiation Therapy, Shanghai, China 201321

Abstract — **The first patient treated with fast neutron teletherapy was in 1938. Less than stellar results were achieved with the first clinical trials but re-evaluations of the trials spurred new clinical trials that began in the late 1960's. With this renewed interest, many new facilities around the world were built and began treating patients between 1970 and 1995. This article reviews and compares some of the technology used at those facilities including: sources of neutrons, gantries, radiation head components and beam shaping, beam characteristics, and treatment planning methods.**

Keywords — **fast, neutron, teletherapy, history**

I. Introduction

In 1932, James Chadwick discovered a new form of radiation, the neutron. Physicians and physicists, always looking for a better form of radiation with which to treat their patients, took interest. Eventually, three types of neutron therapy were investigated and delivered to patients. Fast neutron teletherapy (FNT) was delivered to patients with external beams of neutrons with maximum energies between 2 and 70 MeV. Neutron brachytherapy (NBT) used neutron emitting sources with energies between 1 and 10 MeV placed intracavitarily, interstitially, or on the surface of a patient. Neutron capture therapy (NCT) used external beams of thermal or epithermal energy neutrons applied to a patient after a biochemical agent with an attached neutron absorbing isotope had been injected into the patient. After the isotope absorbs a neutron, secondary radiation is emitted such as low-energy charged particles or photons. This article briefly reviews the the technology associated with the worldwide expansion of FNT between the years of approximately 1970 and 1995.

The first FNT clinical trial was performed at the University of California - Berkeley by Robert Stone; he reported unsatisfactory results [1]. A later evaluation of the trial suggested that the unknown effects of fractionation was probably the cause of the poor results and a second FNT clinical trial was thus begun at Hammersmith hospital by Mary Catterall [2]. A race to improve radiation therapy using FNT then began with at least 35 institutions around the world treating patients. Table 1 gives a list of facilities known to have treated patients, the primary neutron source reactions, the maximum neutron energies, the types of gantries, the approximate start date of the first patient treatment, and for some of the facilities, the approximate number of patients treated and the date of the last patient total. The facilities in the table are listed approximately by the first patient treatment date for each program but some programs significantly modified or obtained new equipment; in those cases, the newer facilities are listed adjacent to the original facility. Although the exact number of total patients that have been treated worldwide is difficult to obtain, a reasonable estimate from the incomplete and outdated data in table 1 suggests over 30,000 through 2024.

II. Sources, facilities, and accelerators

The four most common types of sources that have been used for FNT are given in table 2. A fission source may be supplied by a nuclear reactor that produces many thermal neutrons that can be converted to fast neutrons using a uranium-235 converter. A fusion source may be supplied by a tube where incident deuterons with energies between 100 and 500 keV are incident on a tritium target. Deuterons can be accelerated by a cyclotron or linac and impinged upon a beryllium-9 target resulting in either a stripping or breakup reaction. Lastly, protons accelerated by a cyclotron or linac can be impinged upon a beryllium-9 target resulting in an inelastic interaction.

The FNT sources given above were housed predominantly in five types of facilities:

- parasitic to a research nuclear reactor
- a dedicated fusion tube in a medical center
- parasitic to a research cyclotron
- parasitic to a research linear accelerator
- a dedicated cyclotron in a medical center

Table 1: List of known FNT facilities that treated patients. In column 4 the letters after the energy represent the type of accelerator used: c ≡ cyclotron, vdg ≡ van de Graff, L ≡ RF linear accelerator, r ≡ nuclear reactor.

Facility, City	**Country**	**Primary Reaction**	**Max. Neutron Energy [MeV]**	**Gantry Types**	**First Patient**	**Est. # of Patients**	**Date of Total**
UCal 1, Berkeley	USA	^{9}Be(d,n)^{10}B	8, c	H	1938	34	1939
UCal 2, Berkeley	USA	^{9}Be(d,n)^{10}B	16, c	H	1939	226	1943
Hammersmith Hospital, London	UK	^{9}Be(d,n)^{10}B	16, c	H	1965	500	1977
NIRS 1, Chiba	Japan	^{9}Be(d,n)^{10}B	2.8, vdg	V	1969	36	1975
NIRS 2, Chiba	Japan	^{9}Be(d,pn)^{9}Be	30, c	V	1975	2,129	1996
SZK Berlin-Buch, Dresden	Germany	^{9}Be(d,n)^{10}B	13.5, c	H	1972	990	1990
Texas A&M U 1	USA	^{9}Be(d,n)^{10}B	16, c	H	1972	incl. below	1973
Texas A&M U 2	USA	^{9}Be(d,pn)^{9}Be	50, c	H	1973	248	1976
MD Anderson, Houston	USA	^{9}Be(p,n)^{9}B	42, c	R, H	1983		1997
NRL (MANTA), Washington, D. C.	USA	^{9}Be(d,pn)^{9}Be	35, c	H	1973	86	1979
U Washington 1, Seattle	USA	^{9}Be(d,pn)^{9}Be	22, c	H	1973	incl. below	1984
U Washington 2, Seattle	USA	^{9}Be(p,n)^{9}B	50.5, c	R	1984	3,500	2023
Netherlands Cancer Inst., Amsterdam	Netherlands	^{3}H(d,n)^{4}He	14	R	1975	435	1981
Fermilab, Chicago	USA	^{9}Be(p,n)^{9}B	66, L	H	1976	3,348	2013
U Hospital Eppendorf, Hamburg	Germany	^{3}H(d,n)^{4}He	14	R	1976	822	1990
Inst. Medical Science, Tokyo	Japan	^{9}Be(d,n)^{10}B	14, c	H	1976	458	1991
NASA Lewis (GLANTA), Cleveland	USA	^{9}Be(d,pn)^{9}Be	25, c	H, V	1977		1982
NASA Lewis (GLANTA), Cleveland	USA	^{9}Be(p,n)^{9}B	43, c	H, V	1982	1,200	1990
U Edinburgh, Edinburgh	UK	^{9}Be(d,n)^{10}B	15, c	R, H	1977	620	1984
Christie Hospital, Manchester	UK	^{3}H(d,n)^{4}He	14	R	1977		
Belvedere Hospital, Glasgow	UK	^{3}H(d,n)^{4}He	14	R	1977		
U Heidelberg, Heidelberg	Germany	^{3}H(d,n)^{4}He	14	R	1977	441	1990
U Essen, Essen	Germany	^{9}Be(d,n)^{10}B	14	R	1978	769	2006
Catholic U, Louvain-la-Neuve	Belgium	^{9}Be(d,pn)^{9}Be	50, c	V	1978	incl. below	1981
Catholic U, Louvain-la-Neuve	Belgium	^{9}Be(p,n)^{9}B	65, c	V, H	1982	1,870	2001
INP, Krakow	Poland	^{9}Be(d,n)^{10}B	12.5, c	H	1978	202	1987
U Chicago, Chicago	USA	^{2}H(d,n)^{3}H	11	H	1979		
CHR, Orleans	France	^{9}Be(d,pn)^{9}Be	34, c	V	1981	1,729	2007
Fox Chase, Philadelphia	USA	^{3}H(d,n)^{4}He	14	R	1981	11	1990
King Faisal, Riyadh	Saudi Arabia	^{9}Be(p,n)^{9}B	26.5, c	R	1984	119	1996
NRMC, Tomsk	Russia	^{9}Be(d,n)^{10}B	13.6, c	H	1984	1,500	2022
WWU, Münster	Germany	^{3}H(d,n)^{4}He	14	R	1985	269	1995
RENT, Munich	Germany	n_{th}(^{235}U,n)	mean ˜1.9, r	H	1985	715	2000
FRM II, Munich	Germany	n_{th}(^{235}U,n)	mean ˜ 1.9, r	H	2007	124	2013
MRRC, Obninsk	Russia	n_{th}(^{235}U,n)	mean ˜ 1, r	H	1985	500	2002
UCLA, Los Angeles	USA	^{9}Be(p,n)^{9}B	46, c	R, H	1986		
Korea Cancer Center, Seoul	Korea	^{9}Be(p,n)^{9}B	50.5, c	R	1986	310	1994
MRC, Clatterbridge	UK	^{9}Be(p,n)^{9}B	62.5, c	R	1987	384	1995
iThemba Labs, Faure	South Africa	^{9}Be(p,n)^{9}B	66, c	R	1988	1,788	2015
RFNC, Chelyabinsk	Russia	n_{th}(^{235}U,n)	mean ˜ 1.9, r	H	1988	1,300	2022
IHEP, Beijing	China	^{9}Be(d,pn)^{9}Be	35.5, L	H	1991	485	2001
Wayne State U, Detroit	USA	^{9}Be(d,pn)^{9}Be	48.5, c	R	1991	2,251	2025
Centre Antoine-Lacassagne, Nice	France	^{9}Be(p,n)^{9}B	60, c	V	1993	57	2001
			Total from table			**> 29,456**	

Table 2: Most common types of FNT sources.

Type	**Form**	**Description**
fission	nuclear reactor	n_{th} with ^{235}U converter
fusion	tube	^{3}H(d,n)^{4}He incident deuterons, 100 - 500 keV
stripping or breakup of light ions	cyclotron or linac	^{9}Be(d,n)^{10}B, ^{9}Be(d,pn)^{9}Be incident deuterons, 2 - 50 MeV
inelastic reactions	cyclotron or linac	^{9}Be(p,n)^{9}B incident protons, 26 - 66 MeV

Only three of the facilities listed in table 1 are known to have used nuclear reactors for FNT. A normal light-water moderated reactor is a poor source of fast neutrons with the fluence rate of neutrons above 1 MeV being about 10^{-8} that of the thermal neutrons [3]. For FNT, a highly enriched (example 93%) U-235 conversion target can be placed near the reactor core. When a thermal neutron is captured by a U-235 nucleus, fission occurs with the emission of about two fast neutrons. A transport channel can funnel the fast neutrons out of the pool and through its shielding. Figure 1 is a conceptual diagram showing the basic components of a generic FNT facility that uses a "swimming pool" type research nuclear reactor. Many gamma rays are also emitted but a filter of lead or bismuth can be used to attenuate many of the low-energy ones. The maximum neutron energy at the RENT facility in Munich, Germany was about 10 MeV, the mean energy of the neutron spectrum was about 2 MeV, and the most probable energy was about 0.65 MeV [3]. A new research reactor (FRM) was built in Munich to replace the original facility. The treatment room at the new facility contained a motorized patient positioner and a multi-leaf collimator (MLC) to shape the irradiation field [4]. The maximum field size at the new facility was 200 mm by 300 mm.

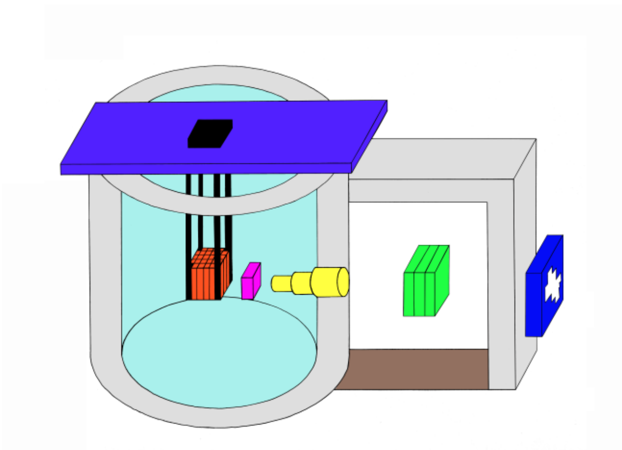

Fig. 1 Conceptual diagram of a research "swimming pool" nuclear reactor used for FNT showing the major components. Components by color: gray - shielding; red - reactor core; black - core support; aqua - water; purple - support crane platform; magenta - U-235 conversion target; yellow - fast neutron transport channel; green - beam filters; blue - MLC, brown: floor of equipment room.

The fusion-based systems typically gave a nearly monoenergetic beam of neutrons with an energy near 14 MeV with the energy depending slightly on the configurations of the ion source, the target, and collimators [5]. One method of producing fusion used a continuously pumped assembly in which a deuterium ion beam was incident upon a rotating metal hydride coated target with a heat-conducting backing. A second method used a sealed tube in which a mixed ion beam of deuterium and tritium was accelerated onto a tritium-coated target such as titanium. A third method accelerated a deuterium beam onto a vessel containing pressurized tritium gas. Fusion systems were supplied by six different companies: Haefely, Marconi-Elliott, Phillips, Radiation Dynamics, Texas Nuclear, and The Cyclotron Corporation (TCC).

Key advantages of fusion-based systems were that the accelerator and gantry were both small. Most rotating gantries for fusion-based systems used a slewing ring with a gooseneck style arm to support a radiation head somewhat larger than the head for a typical cobalt-60 unit. A few used a gantry and radiation head configuration similar to those that were used with some of the larger megavoltage betatron installations where the radiation head rotated as the patient positioner moved laterally and vertically to align the patient with the beam. Disadvantages of fusion-based systems were that they produced low dose rates (5 - 20 cGy/min), had relatively low penetrating beams (slightly less than a cobalt-60 beam), had wide lateral penumbras, and the tubes had limited lifetimes (75 to 1,000 beam hours) requiring frequent replacement. All but one of the fusion-based systems that treated patients were installed into medical facilities in Europe. Figure 2 is a picture of a TCC isocentric slewing ring gantry with the bottom part of the radiation head pulled down showing the tube inside. Figure 3(L) shows a floorplan for a facility based upon the TCC equipment. The size is comparable to a conventional megavoltage x ray room. Figure 3(R) shows a vertical cross-section through the gantry isocenter. Only a small depression in the floor was required to accommodate the radiation head while it was rotated by the gantry. The installation at Fox Chase treated very few patients as the tube needed to be replaced shortly after the system commissioning was finished but, by then, TCC had gone bankrupt and new tubes were unavailable.

Several of the early cyclotron-based facilities parasitically used research cyclotrons. When the University of Texas M. D. Anderson Cancer Center (MDA) in Houston, Texas, U.S.A. wanted to start a clinical trial of FNT, they found a cyclotron at the Texas Agriculture and Mechanical University Variable Energy Cyclotron (TAMVEC) facility, in College Station, Texas, about 100 miles away. This cyclotron had a pole tip diameter of 88 inches and could accelerate light ions with atomic numbers from 1 to 10 (protons to neon). A decision was made to use the $^{9}Be(d,n)^{10}B$ stripping reaction to generate a beam of fast neutrons. From 1972 to 1973, 16 MeV deuterons were used but during 1973 the deuteron energy was switched to 50 MeV to provide a higher energy neutron spectrum predominantly via the $^{9}Be(d,pn)^{9}Be$ breakup reaction [7-9]. Figure 4 shows the floorplan of the TAMVEC facility.

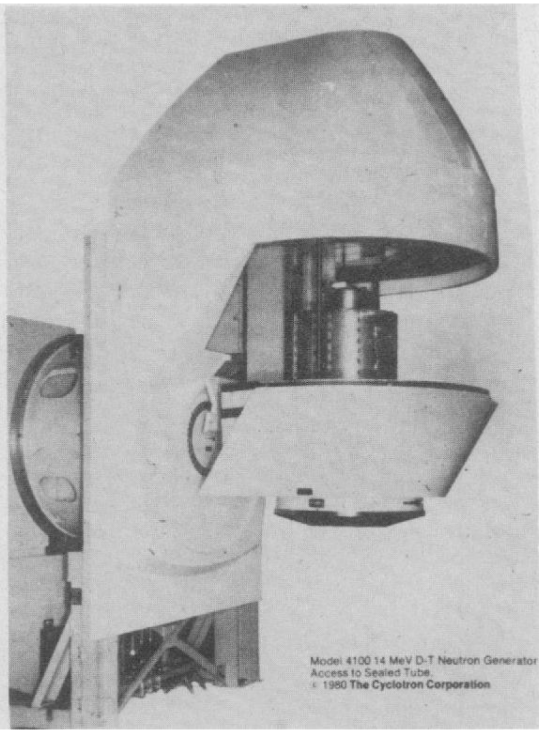

Fig. 2 Picture of gantry and opened radiation head for TCC based fusion source. Reprinted from Bloch et al. [6] with permission from IEEE.

The fixed horizontal beam configuration, low-energy neutron spectrum, lack of available beam time, and large distance from the hospital to the TAMVEC facility suggested that a dedicated medical facility be built in Houston, preferably within the hospital. During 1978 the National Cancer Institute (NCI) issued a Request for Proposal (RFP) for institutions across the USA to propose FNT facilities. In 1979, MDA received one of three 10-year contracts to design, develop, and build, hospital-based neutron therapy facilities and conduct phase III clinical trials [10]. The company chosen to provide and install the equipment at MDA was TCC [11]. This company also produced and installed equipment at several other FNT facilities around the world, both cyclotron-based and fusion-based. Figure 5 shows a floorplan of the dedicated medical facility that was housed in the basement of the MDA hospital adjacent to other radiotherapy equipment including the 32 MeV Sagittaire electron / x ray system. The extracted beam could be sent to one treatment room housing a stationary gantry to provide a horizontal neutron beam, a second treatment room housing a ± 110° rotating gantry, or a room with multiple targets for isotope production. The facility also included a "hotlab" for processing the isotopes and drugs, a cyclotron control room, and a treatment control room. Descriptions of the facility and commissioning of the treatment beams were given by Almond et al. [13] and Horton et al. [14].

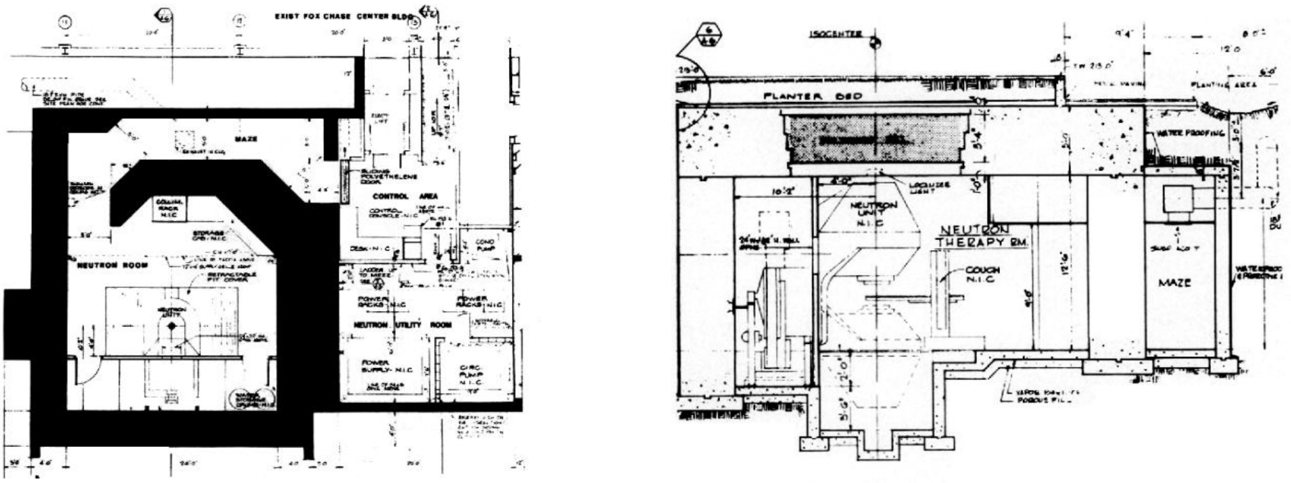

Fig. 3 (L) Floorplan for the Fox Chase facility in Philadelphia, Pennsylvania, U.S.A. based upon TCC equipment. (R) Vertical cross-section through the gantry isocenter. Reprinted from Bloch et al. [6] with permission from IEEE.

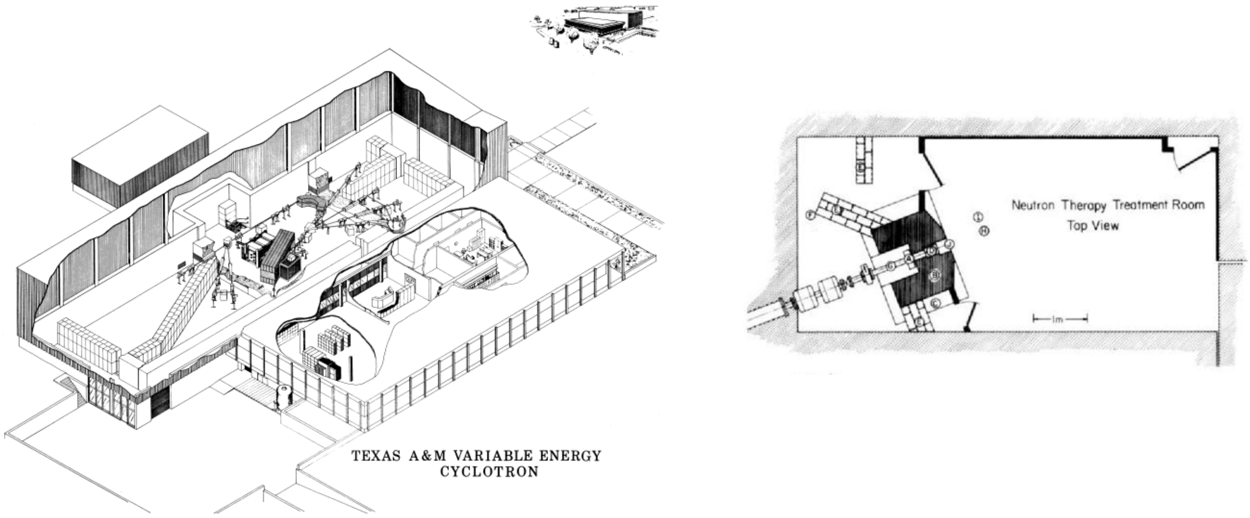

Fig. 4 Parasitic research cyclotron facility at TAMVEC. Reproduced from TAMVEC facility description document.

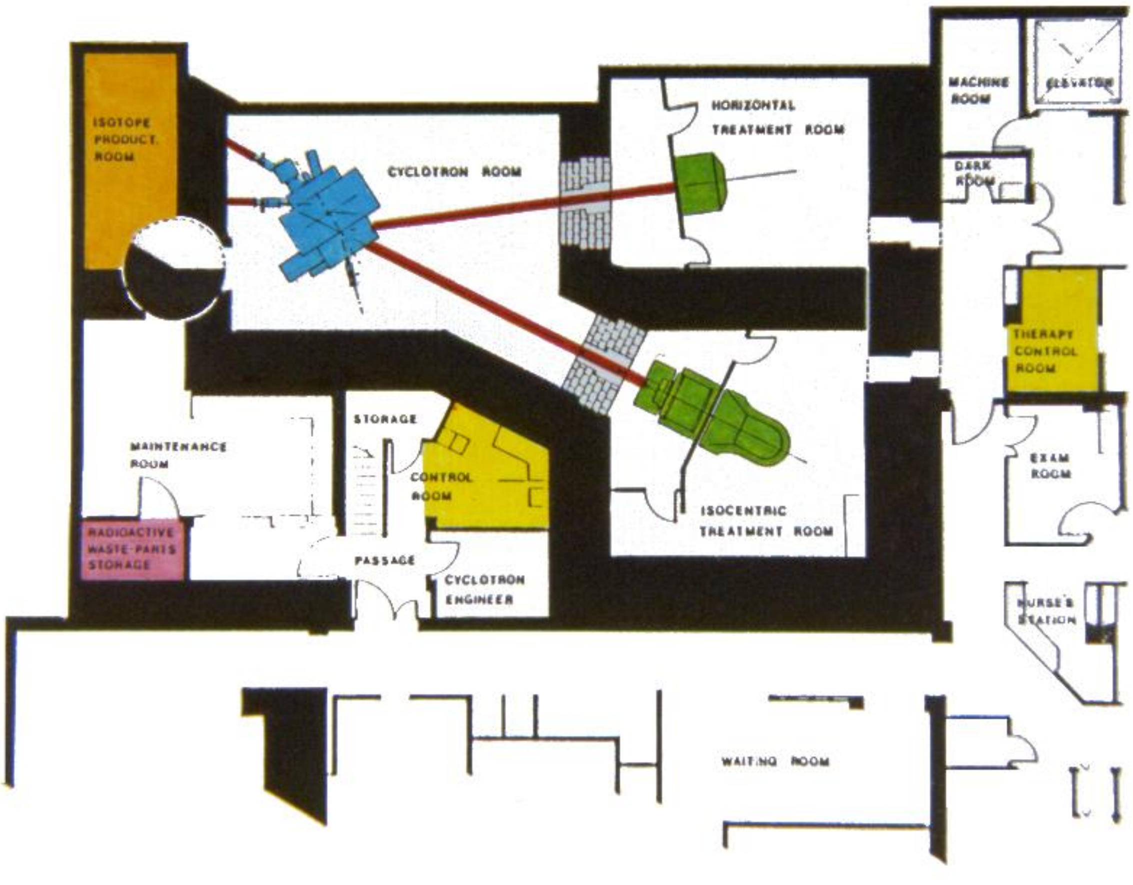

Fig. 5 Floorplan of dedicated medical cyclotron facility at MDA. One sliding shielding door was shared between the two FNT treatment rooms. One rotating shielding door allowed access from the cyclotron control room to either the cyclotron room or the isotope production room. Reproduced from Moyers [12].

Except for one parasitic linac based facility, all facilities producing neutron beams with energies higher than 16 MeV utilized cyclotron accelerators. Some cyclotrons accelerated positively charged ions while others accelerated negatively charged ions. Some cyclotrons could extract beam at multiple energies while others at only one. The system chosen for MDA was an isochronous cyclotron that accelerated negatively charged ions. Charge stripping foils were used to extract the beam from different energy orbits through one of five different extraction ports. Figure 6 shows the inside of the MDA TCC cyclotron while figure 7 shows a schematic of the inside. Figure 8 illustrates the positions of the foils on different orbits and extraction beam paths.

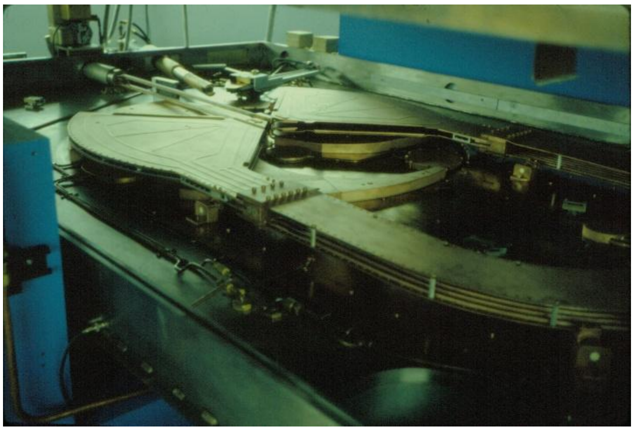

Fig. 6 Picture of inside of TCC cyclotron showing RF electrodes, pole tips, ion source, and beam diagnostics.

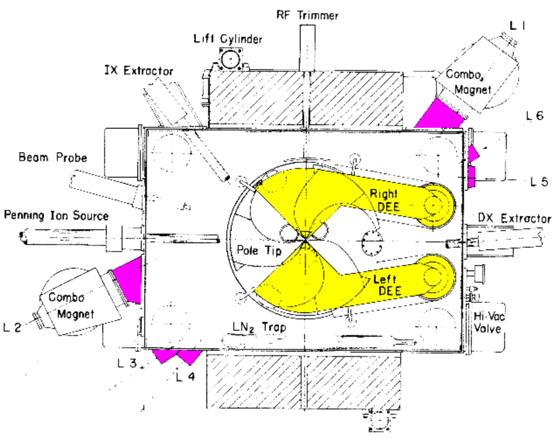

Fig. 7 Diagram of TCC cyclotron layout.

Shortly after the installation of the cyclotron and associated equipment at MDA, TCC went bankrupt and technical support decreased. This resulted in significant downtime but several upgrades improved the performance for the clinic [15]. At one point, a large breakdown occurred and the equipment was out of service for 1.5 years. After much investigation, it was discovered that internal stray radiation beam stopper strips attached to the inside of the cyclotron were approximately one quarter of the wavelength of the applied radiofrequency (RF) resulting in large power losses and strain on the equipment. During this time, the NCI arranged for some of the experiments described in section V to be performed at UCLA which had also received NCI funding to build a neutron facility using the same company. Eventually the MDA cyclotron was put back into working order. In 1998, however, the cyclotron was dismantled, transferred to Denton, Texas, and reassembled where it would only be used for radioisotope production [16].

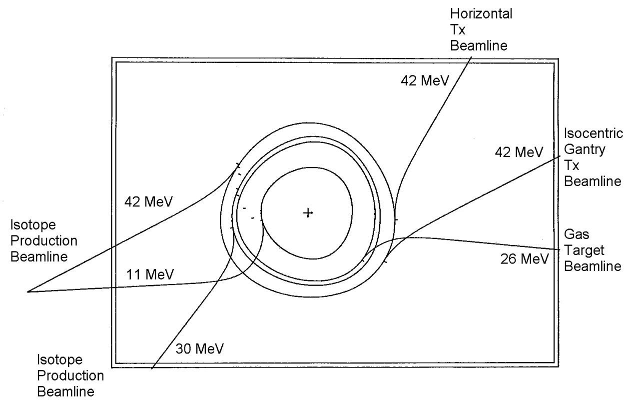

Fig. 8 Diagram showing stripping foils paced at different locations around the cyclotron to intercept different energy orbits and extract beam through one of five different extraction ports.

Another commercial cyclotron used for FNT was produced by Scanditronix and installed in Seattle, Washington in the U. S. A. and in Clatterbridge in the U. K. This cyclotron accelerated positive ions and extracted beam through a magnetically shielded channel. A diagram of the cyclotron is shown in figure 9.

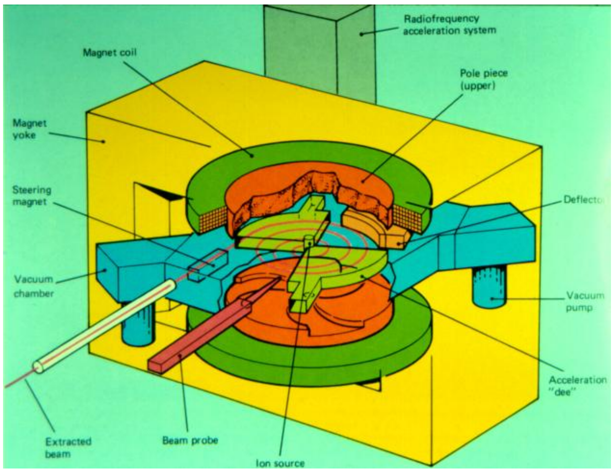

Fig. 9 Diagram of positive ion cyclotron produced by Scanditronix. Reproduced from Scanditronix MC series cyclotrons brochure.

An interesting cyclotron that was used parasitically for FNT was the separated-sector cyclotron at the iThemba labs in South Africa seen in figure 10. This cyclotron accelerated protons for FNT to 66 MeV, for proton therapy to 200 MeV, and for isotope production to several other energies. For this positive ion cyclotron, the energy changes were achieved by changing the magnetic field of the main magnets. For the switch from 200 MeV to 66 MeV, the change required about two hours before becoming stable enough for treatment.

Fig. 10 Separated-sector cyclotron at iThemba Labs near Faure, South Africa. Yellow objects are the C-shaped bending magnets.

III. Gantries for cyclotron-based facilities

To produce high energy neutron beams with a cyclotron, the ion beam is first accelerated and then transported to a radiation head attached to a gantry where it is converted to neutrons. Many of the early cyclotron facilities used a stationary gantry with either horizontal, vertical, or both beam directions. During the trial at TAMVEC, patients could only be treated two days a week, Tuesday and Thursday, and therefore most neutron treatments were combined with megavoltage x ray beams. Due to the beamline having a stationary horizontal direction, pelvic patients were treated standing. The average anterior-posterior diameter for these patients when treated supine or prone with 25 MV photons was 20.2 cm but, when the same patients were treated in a standing position with FNT, the diameter was 25.6 cm resulting in inferior dose distributions [17]. Another consequence of this positioning is that when a patient was lying, the intestine tended to move into the upper abdomen whereas, when standing, the intestine tended to shift into the lower abdomen and pelvis. These issues confounded having a "clean" clinical trial of neutrons versus photons.

Figures 11(L) and 11(R) show a configurable rotating patient positioner for seated and standing patients respectively in the Fermilab treatment room which had a horizontal gantry. To improve dose calculations for seated or standing patients, Fermilab installed an XCT scanner with a vertical axis to reproduce the position of the patients when treated. Figures 12(L) and 12(C) show the scanner in the raised and lowered positions respectively. Figure 12(R) shows the computer hardware for the scanner.

Fig. 11 Fermilab configurable patient positioner used in combination with horizontal beamline. (L) Configured for seated patients. (R) Configured for standing patients.

Fig. 12 Vertical axis XCT scanner installed at Fermilab. (L) Scanner in raised position. (C) Scanner in lowered position. (R) Scanner computer hardware.

Improvements in FNT dose distributions came with the introduction of rotating gantries. The first generation of rotating gantries for high energy neutrons typically rotated only about ± 100º from the vertical to avoid the need for a large pit in the floor that would make patient set-ups difficult. Figure 13 shows three of these rotating gantries. The target-to-isocenter distance for the MDA gantry was 125 cm. For posterior beams, the patient had to be placed in either prone or decubitus orientations causing some uncertainty in the dose distributions for multiple beam direction plans. A second generation of rotating gantries was built by Scanditronix that rotated a full 360º. Two of these are shown in figure 14. All of the above-mentioned rotating gantries used a slewing ring near the axis of rotation and a goose-neck configured beamline to deliver beam to the radiation head [18].

One of the last FNT installations was at Wayne State University in Detroit, Michigan, U. S. A. This facility had a superconducting cyclotron mounted directly to a 360º rotating gantry without the need for an ion transport beamline [19]. This cyclotron accelerated deuterons onto a beryllium target. Figure 15(L) is a conceptual diagram of the double ring gantry showing the basic components while figure 15(R) shows the patient enclosure during preparation for treatment.

Fig. 13 Rotating gantries with approximately ± 100º rotation from the vertical. (L) Essen, Germany. (C) MDA. (R) UCLA.

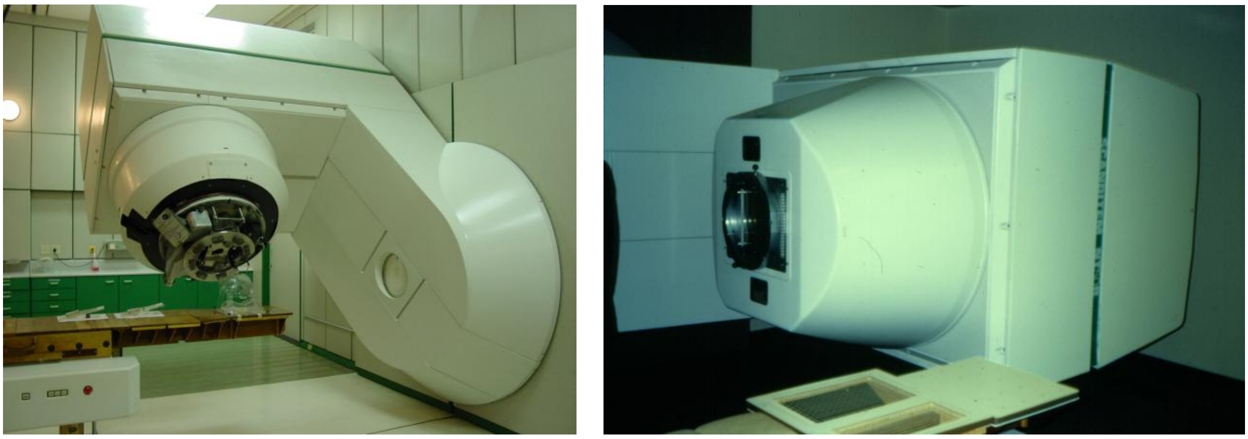

Fig. 14 Examples of fully rotating slewing ring gantries. (L) iThemba Labs. (R) University of Washington. For beams pointing upwards, floor panels would shift to the side allowing the radiation head to be rotated into a pit below the level of the false floor. The major difference between the two gantries is the shape of the collimator housing.

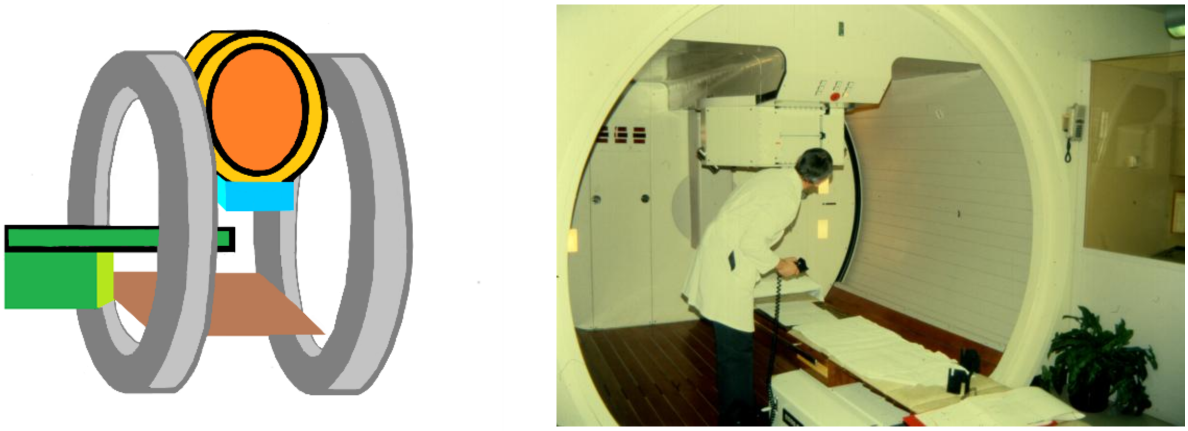

Fig. 15 Fully rotating double ring gantry for a superconducting cyclotron. (L) Conceptual diagram showing major components: gray - front and back rotating rings; orange and yellow - superconducting cyclotron mounted between front and back rings; blue - collimator assembly; green - patient positioner; brown - false floor. (R) Picture of patient enclosure.

IV. Radiation head components and beam shaping

The arrangement and composition of parts within the radiation head from each manufacturer is different but typically contain some similar basic components. Figure 16 is a diagram of the inside of the MDA radiation head mounted on the rotating gantry. It will be used as an example to illustrate the different components.

An important part of the radiation head is the neutron conversion target assembly. Figures 17(L) and 17(R) show pictures of the MDA target assembly and a diagram of its components respectively. The upper section contains four steering slits that intercept the edges of the light ion beam before it impinges upon the neutron conversion target. If the light ion beam is delivered off-center, feedback signals are sent to steer the beam back to center. The intense light ion beam carries a lot of power and thus water cooling is provided for the slits. The lower part of the assembly houses the beryllium slab target for converting the light ions to neutrons. The beryllium slab is also equipped with cooling water. When the light ion beam strikes the beryllium, different energy neutrons are produced in different directions. Moyers [12] reviewed various studies of thin target data for incident protons and developed a model for a thin target neutron spectrum in the forward direction. Figure 18 shows several thin target spectrums calculated for different incident energies.

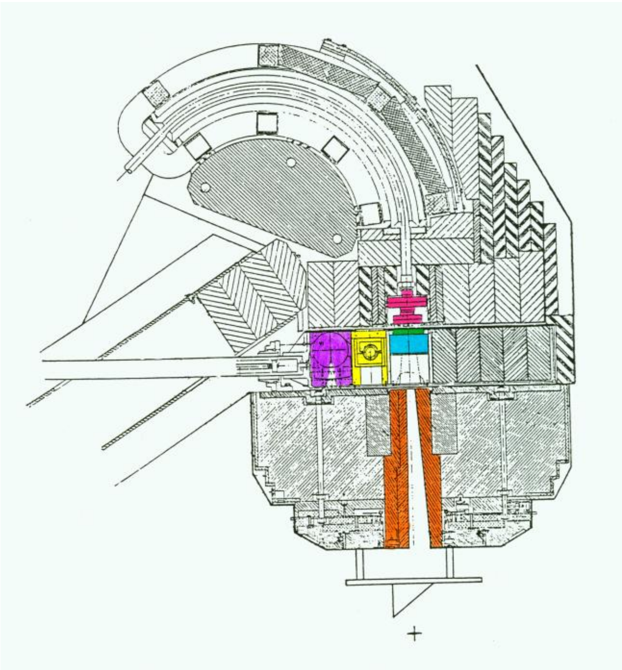

Fig. 16 Diagram showing the components of the MDA radiation head. The different styles of cross-hatched regions represent different kinds of shielding. The target assembly that includes steering slits is colored magenta. A 33 mm thick polyethylene hardening filter is colored green. The monitor ionization chamber assembly is colored blue. The exchangeable Benelex collimator is colored orange. A light source assembly is colored yellow. An in-line x ray tube is colored purple. Beneath the radiation head is a tray to which a wedge filter may be mounted. Reproduced from Moyers [12].

Obviously, the number of neutrons produced from a thin target is small so thick beryllium targets are used to increase the dose rate delivered to patients. Figure 19 shows the bottom half of the target assembly shown in figure 17 but taken apart to reveal the beryllium target slab, copper heat conductor, and inlet and outlet water channels. To reduce the number of low-energy neutrons produced, the thickness of the beryllium target is less than the range of the protons in beryllium, a so-called intermediate thickness target. After passing through the beryllium, the protons stop in the copper which has a smaller neutron production cross-section than does beryllium. Nevertheless, some low-energy neutrons are still produced. The UCLA target assembly, seen as a diagram in figure 20, is similar to the MDA assembly but slightly different. After protons pass through the intermediate thickness target, they enter a slab of graphite that has a much lower cross-section for neutron production than does copper. Copper is still used in the assembly, however, to conduct heat from the beryllium and graphite to the circulating cooling water.

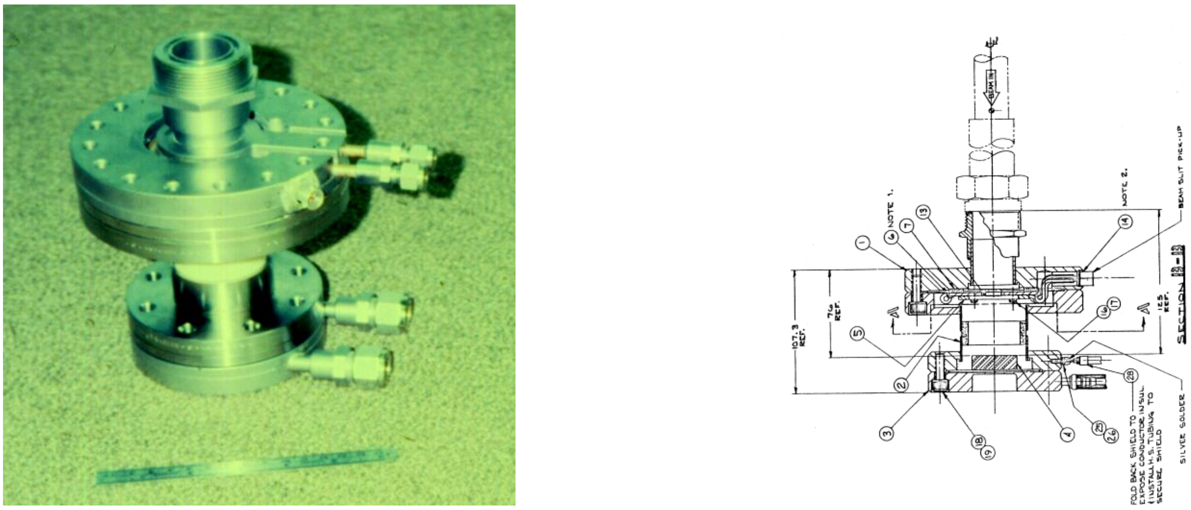

Fig. 17 MDA target assembly. (L) Picture of assembly showing water cooling pipes. (R) Diagram showing assembly components.

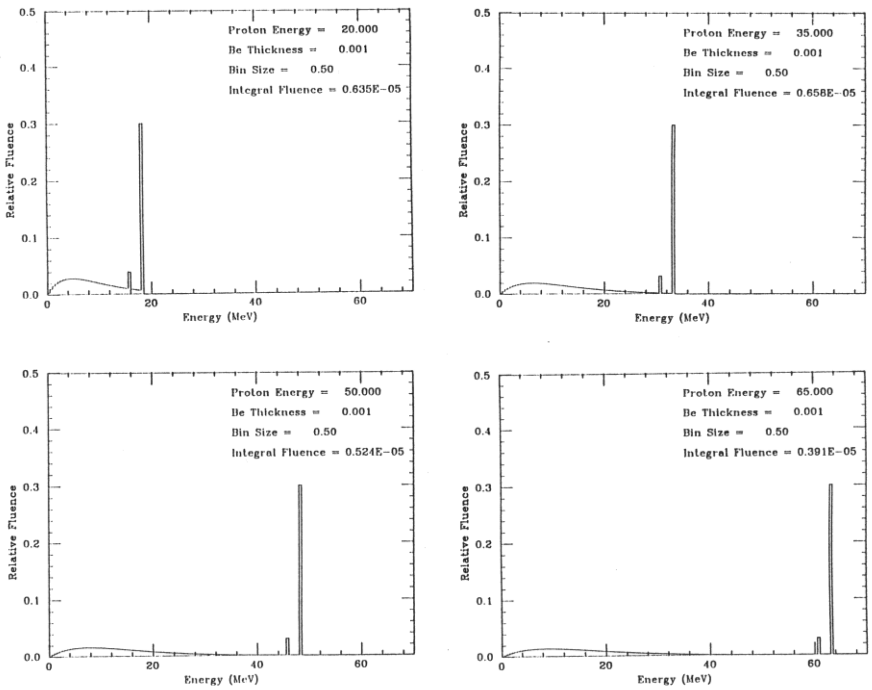

Fig. 18 Neutron production spectrum in the forward direction for different energy proton beams incident on a thin beryllium target. Reproduced from Moyers [12].

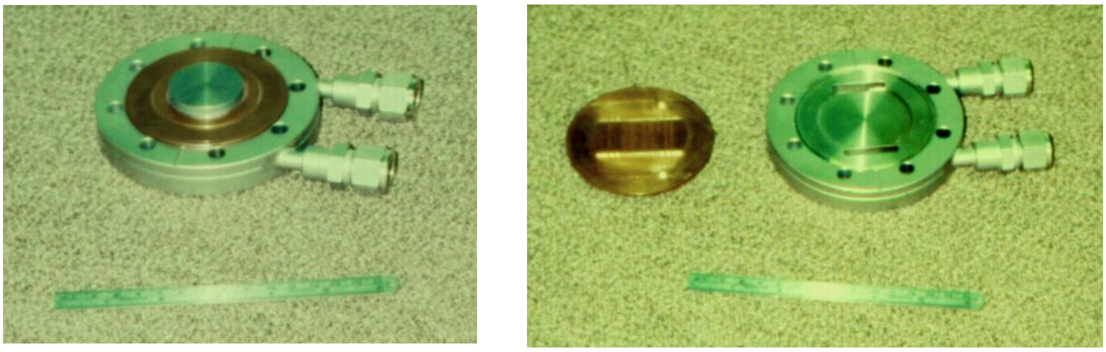

Fig. 19 Beryllium slab target and heat dissipation mechanism. (L) Surface at which the proton beam impinges on the beryllium. (R) Beryllium and copper slabs removed and turned upside down revealing narrow slits in the copper to increase the surface area over which water may flow for cooling.

Just distal to the target assembly is an assembly that houses a hardening filter, neutron beam monitor chambers, and a pre-collimator. Figure 21 is a diagram of this assembly. This assembly is only in place during beam delivery for treatment. At other times, such as during patient set-up, either a light field or x ray tube assembly would be in place. As can be seen in figure 16, this would also place the pre-collimator, that had been exposed to intense radiation, inside a shielded volume of the radiation head thereby reducing exposure of the staff and patient to residual radioactivation.

Table 3 lists the radiation head components for the high-energy neutron facilities that were treating patients during the late 1980s. It is apparent that no two facilities were the same. Figure 22 compares calculated neutron spectrums in the forward direction for four of these facilities. These spectrums were calculated by summing many thin target neutron spectrums that were generated at multiple depths as the proton beam traversed each component of the target assembly and then attenuating the neutrons in each energy bin by the thickness of the hardening filter. The effects of other components of the radiation head such as the collimators and monitor detectors were not included.

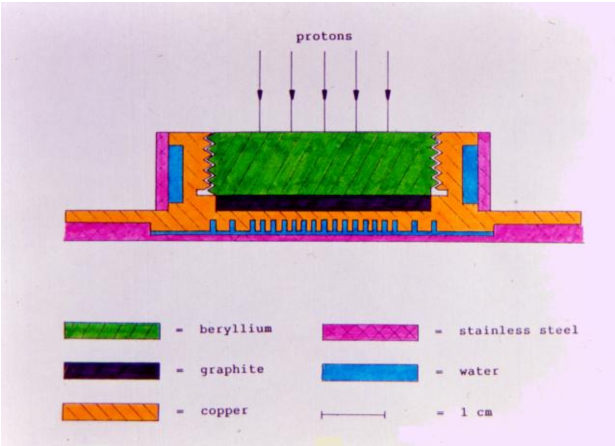

Fig. 20 UCLA neutron conversion target design. Reproduced from Moyers [12] that was modified from an original drawing by Miller (personal communication).

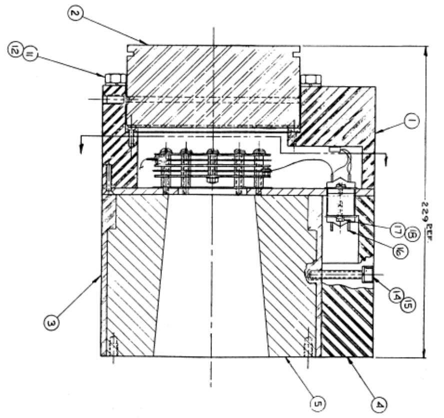

Fig. 21 MDA assembly for holding polyethylene hardening filter (2), monitor ionization chambers, and tungsten pre-collimator (5).

Table 3: Comparison of radiation head components for various high-energy facilities. Reproduced from Moyers [12].

Institution	UT-MDACC Houston Texas	CC Cleveland Ohio	UCLA Los Angeles California	UW Seattle Washington	MRC Merseyside UK	UCL Louvain Belgium	MINTF Batavia Illinois	NAC Faure S. Africa
Proton Energy	41.9 MeV	43 Mev	46 MeV	49.6 MeV	62 MeV	65 MeV	66 MeV	66 MeV
Beryllium	0.6 cm (15 MeV)	0.79 cm (22 MeV)	1.00 cm (26 MeV)	0.9 cm (24.6 MeV)	1.78 cm (36 MeV)	1.7 cm (35 MeV)	2.21 cm (49 MeV)	1.96 cm (40 MeV)
Backstop 1	copper	water	graphite 0.23 cm	copper 0.055 cm	copper 0.6 cm	carbon 0.85 cm	gold 0.05 cm	
Backstop 2	water		copper	water 0.1 cm	water	brass 0.4 cm		
Backstop 3			water	graphite 0.25 cm				
Hardening Filter	C_2H_4 3.3 cm	none	none	none	none	C_2H_4 2.0 cm		C_2H_4 2.5 cm
Flattening Filter	Teflon	none	none	Fe 2.3 cm CAX	Fe			steel
Collimator	Benelex inserts 92.0 cm	WEP inserts	Fe roman square 108.0 cm	Fe / C_2H_4(B) multi-leaf 111.0 cm	Fe / C_2H_4(B) book ends	Fe / epoxy(B) inserts	cement / C_2H_4 inserts 109 cm	Fe / C_2H_4(B) book ends 115 cm
Wedge	Teflon		iron		tungsten		tungsten	
Isocenter	125.0 cm $\pm 100°$	125.0 cm	150.0 cm $\pm 95°$	150.0 cm $\pm 185°$	150 cm $\pm 185°$	162.5 fixed vert.	153.2 cm fixed horiz.	150 cm $\pm 185°$

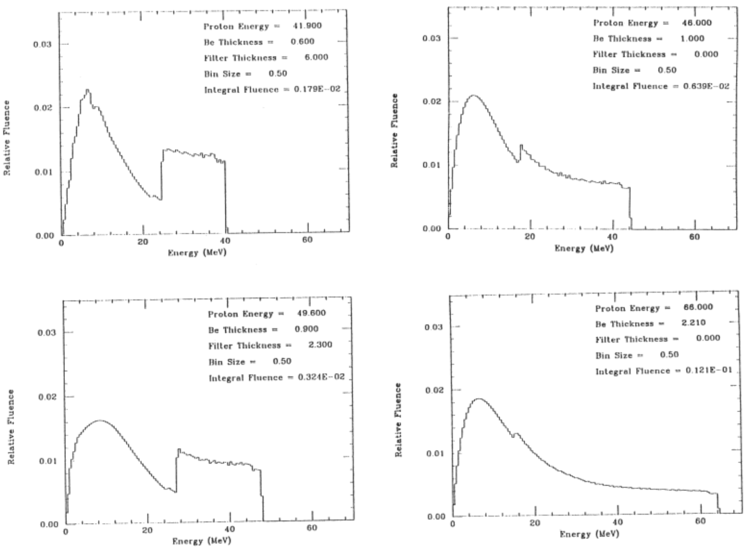

Fig. 22 Calculated thick target neutron spectrums for various high-energy FNT facilities. (TL) MDA. (TR) UCLA. (c) LL. (LR) Fermilab. Reproduced from Moyers [12].

One drawback of early FNT facilities that possibly impacted treatment results was the type of collimation. Unlike for x rays, lead and tungsten are not good attenuators for neutrons. Collimators thus need to be made from a lower atomic number material but generally these materials are less dense requiring them to be quite long. The material chosen for the collimators at MDA and several other facilities was a pressed wood called Benelex®. An inventory of fixed cone collimators was provided to make rectangular field sizes. Occasionally a tungsten block could be added to provide corner blocking. Figure 23(L) shows a single collimator cone while figure 23(R) shows a cabinet with an inventory of collimator cones. The field uniformity of the raw beam was generally good except near the field edge. Each cone was thus provided with a Teflon flattening filter to reduce the neutron fluence in the center of the field to compensate for out-scattered neutrons near the edges of the field. Figure 24 shows three flattening filters that were inserted into the distal ends of the different cones. Some other facilities used shaped steel flattening filters upstream of the collimators.

Fig. 23 (L) Single Benelex collimator cone at MDA. Length of collimator was 92 cm.
(R) Cabinet with inventory of collimator cones for different field sizes.

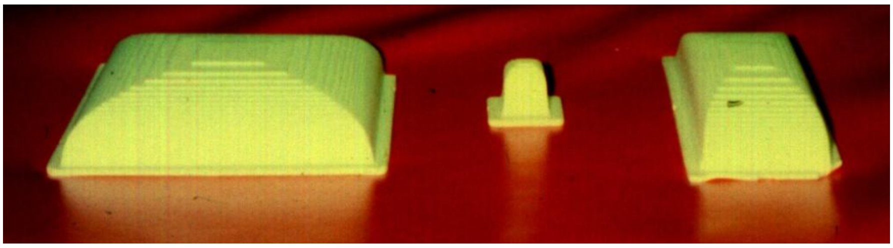

Fig. 24 Teflon flattening filters for different field sizes. The filters were inserted into the patient end of the collimator cones.

A different composition of fixed cones was used at Fermilab. The cones at that facility were composed of a mix of concrete and polyethylene as seen in figure 25. Another material that was used for fix cones was water extended polyester (WEP). Cones of WEP were used at the NASA Lewis Lab in Cleveland in which staff from the Great Lakes Neutron Therapy Association (GLANTA) treated patients.

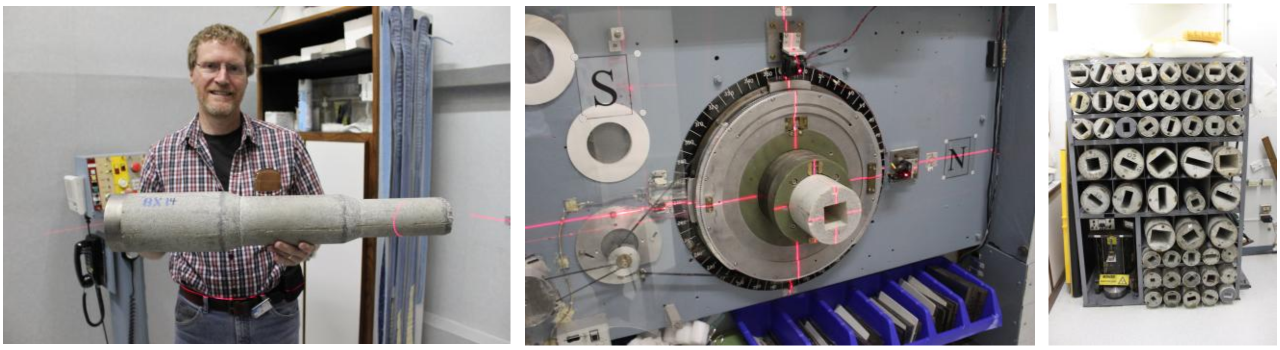

Fig. 25 Fixed cones used at Fermilab constructed of a mix of concrete and polyethylene. (L) Single cone held by Thomas Kroc. (C) Cone installed in radiation head. (R) Inventory of cones for different field sizes.

A significant advance in collimation occurred with the opening of the UCLA facility. This facility had a roman jaw style of collimator that could provide continuously adjustable rectangular field sizes. A high-density material was chosen to reduce the overall length and iron was chosen over other materials due to its reduced radioactivation cross-section. Figure 26 shows the jaws in the open and closed configurations.

Another collimation advance was able to provide irregular field shapes. At Wayne State University (WSU), a multi-rod collimator was devised [20]. This device consisted of 12,000 tungsten rods. The shape of the field was made by first cutting Styrofoam blocks to the desired shape, inserting the blocks against the rods and pushing them into place in the beam path, and then locking the rods so they would not move while rotating the gantry. Figure 27 shows insertion of the Styrofoam rod array shaper and a field shape that can be produced.

At the iThemba Labs, an irregular field shape was made by placing an array of collimation slabs thick enough to significantly attenuate the beam into the beam path. These slabs, called blades, were used similarly to the rods at WSU; the blocks were first moved manually and then locked into place. The blades were backed up by conventional block jaws. Figure 28(L) shows the multi-blade array. Figure 28(R) shows a reverse Beam's Eye View of an MLC similar to the one installed at the University of Washington (UW). The shape of the opening of the MLC was programmed and moved into place electronically. For better neutron attenuation, the MLC leaves at some facilities had disks of borated polyethylene strategically placed into multiple holes of each leaf [21].

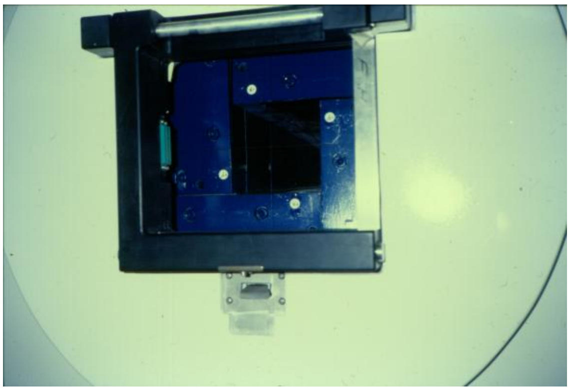
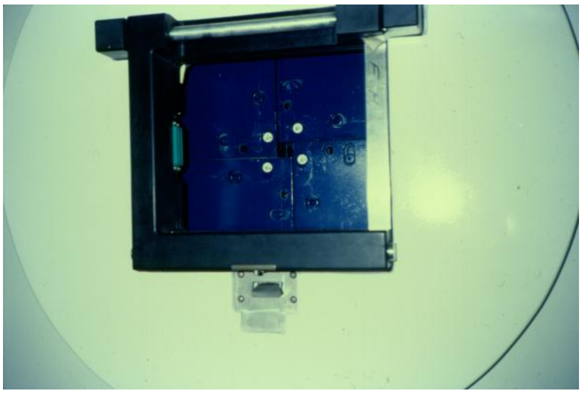

Fig. 26 Pictures of distal end of roman jaws type collimator installed at UCLA. (L) Opened to fullest extent that projects a neutron field with a size of 200 mm by 200 mm at the isocenter. (R) Closed to fullest extent that projects a neutron field with a size of 40 mm by 40 mm at the isocenter.


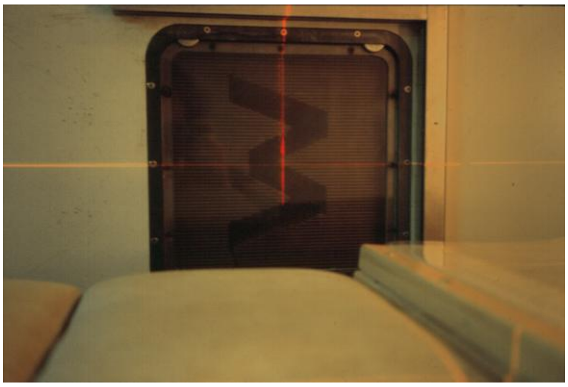

Fig. 27 Tungsten rod array for patient-specific collimation at WSU. (L) Richard Maughan inserting cut Styrofoam blocks used to move the rods into place. (R) A reverse beam's eye view of the tungsten rods after having been moved into place.

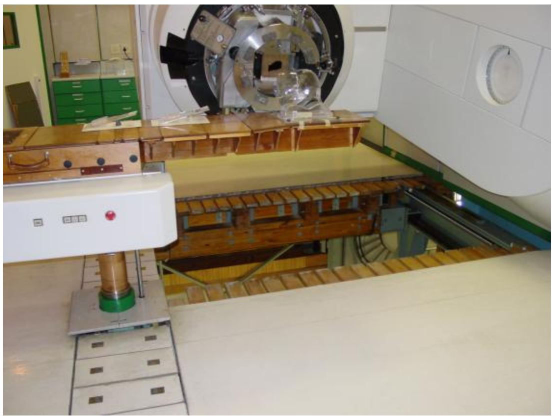
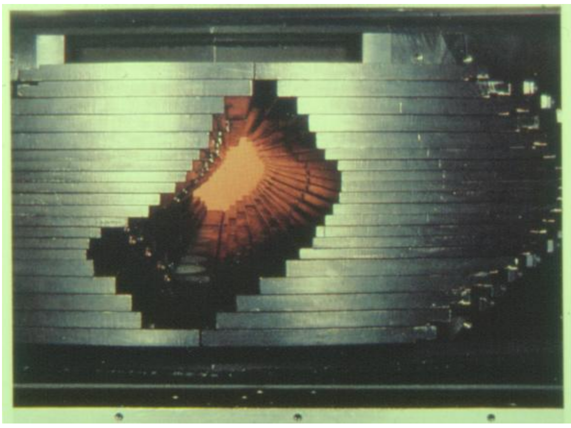

Fig. 28 (L) Multi-blade collimator at iThemba Labs. Note the retractable false floor to allow gantry rotation. The floor and patient positioner top were made of wood to reduce radioactivation. (R) Programmable multi-leaf collimator at UW. Reproduced from Scanditronix MC series cyclotrons brochure.

V. 3D DOSE CALCULATIONS FOR TREATMENT PLANNING

During the 1970's and 1980's, computerized calculation methods for FNT relied on traditional megavoltage x ray (MVX) methods such as: matrix methods (cartesian, polar, fan-line / depth-line, decrement lines for rectangular fields; parameterized generating functions; sector integration (TAR0 + SAR); and pencil beams (that were then just starting to be used). Unfortunately, these methods did not account well for the neutron spectrum, neutron scatter, and contaminating photons. Furthermore, computed tomography scans using x rays (XCT) did not provide sufficient data to accurately calculate neutron interactions, especially for determining the effects of heterogeneous tissue. Monte Carlo methods were known but impractical for routine clinical use at that time.

To overcome these inaccuracies, a new calculation method was developed that utilized multiple fast Fourier transform (FFT) convolutions of multiple three-dimensional (3D) Monte Carlo generated kernels [22-23]. This method utilized a three-source model consisting of primary neutrons, scattered neutrons, and photons. Heterogeneities within the patient were considered by ray tracing through the anatomy and performing linear attenuation on the three source spectrums. Two convolution paths were used for each of the three sources as seen in figure 29. One path convolved a water kernel at each voxel while the other path convolved a difference kernel that was the difference between lung and water kernels. The contribution from each was determined by a weighting factor based upon the material at the voxel.

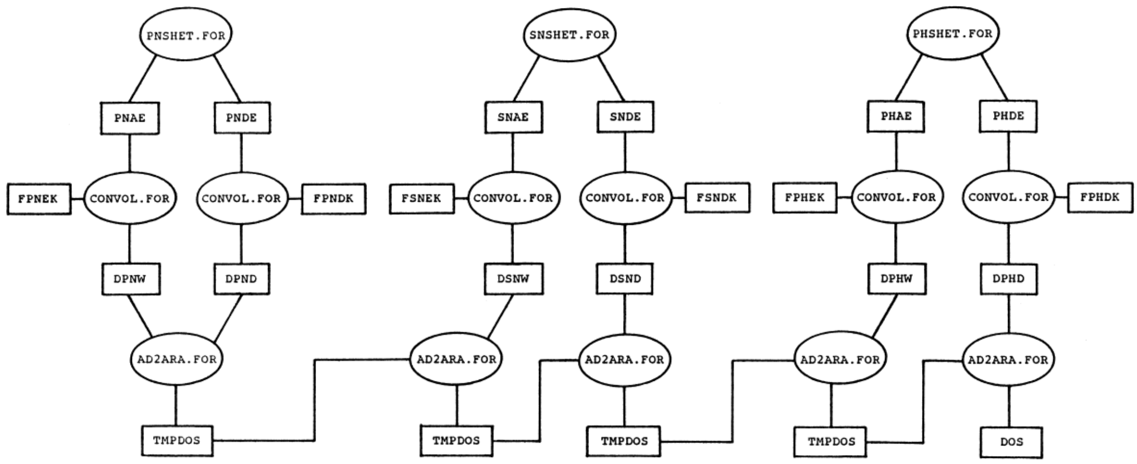

Fig. 29 Program flow for model that considered heterogeneous tissue and three radiation sources. Reproduced from Moyers [12].

The calculated spectrums shown in figure 22 were not sufficiently accurate for the three-source model shown in figure 29 because the flattening filter, hardening filter, and collimation system were not included. Measurements were thus made to refine the spectrums for the three sources. Both narrow and broad field measurements were made with neutron sensitive and neutron insensitive detectors. For these measurements, ionization chambers with walls made of A-150 muscle equivalent plastic and magnesium were used and filled with tissue-equivalent and argon flowing gas respectively. Due to a long breakdown of the cyclotron, the final measurements were made at UCLA that had similar neutron beam delivery equipment to MDA. Figure 30 shows the setup. Three differences between the MDA and UCLA facilities were that UCLA used a roman jaw style of collimator made of iron instead of Benelex cones, the target-to-isocenter distance was 150 cm instead of 125 cm, and the proton energy from the cyclotron was 46 MeV instead of 42 MeV. Figure 31(L) shows the primary and scattered neutron spectrums while figure 31(R) shows the photon spectrum for the UCLA equipment. The contaminating photon spectrum was the world's first published measurement for a high-energy FNT facility.

The off-axis neutron fluence profile was also required for accurate calculations. This was obtained by placing flat copper strips perpendicular to the beam at different distances from the isocenter. The radioactivated strips and a piece of film were then inserted into a film cassette with a scintillation screen to produce a latent image. The film was then developed and scanned to get fluence profiles at different distances from the isocenter. The diameter of a circular pillbox source was then iteratively fit to achieve profiles similar to the activated copper profiles. Figure 32 shows the fluence profile measurement technique, source model, and a fitted profile.

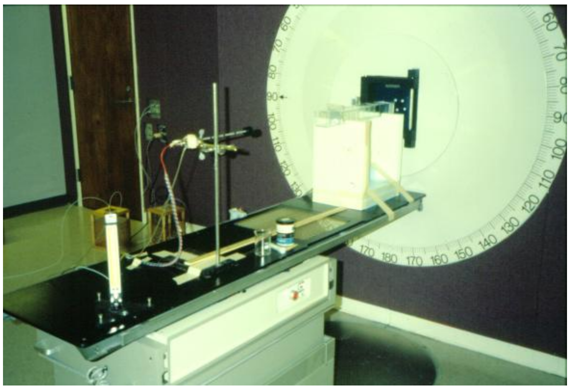

Fig. 30 Setup for measuring attenuation data used in deriving the neutron and photon spectrums. A variable but discrete thickness water column was used to provide narrow beam attenuation. Attenuation measurements were repeated with one chamber being sensitive to both neutrons and photons while a second chamber was sensitive primarily to photons.

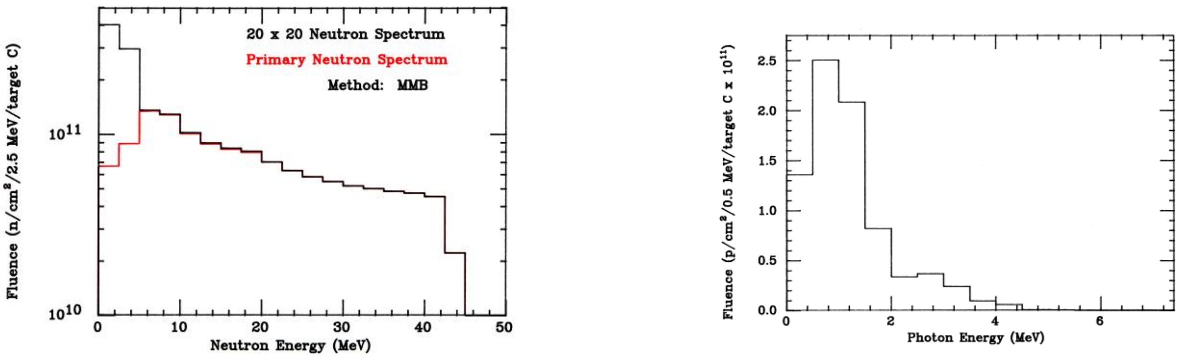

Fig. 31 (L) Primary and scattered neutron spectrums. Figure from Moyers [12]. (R) Photon spectrum. Figure reproduced from Moyers et al. [24] and used with permission of Wiley.

Fig. 32 Measurement and determination of primary neutron source size. (L) Diagram of source model. (C) Copper strips inside film cassette after irradiation of film. (R) Comparison of measured and fit profiles in the lateral penumbra region. Figures (L) and (R) from Moyers [13].

The calculation algorithms were developed using FORTRAN and DEC command language (DCL) on a VAX 750 computer. Initially the FFT codes were taken from Art Boyer and Ed Mok. A grant from Cray Research, however, allowed the calculations to be performed on a Cray X-MP supercomputer with a vector processor located in Austin, Texas (see figure 33). The 3D FFTs sub-routines were then changed to assembly code obtained from the Boeing aircraft company resulting in one of the most efficient programs running on the Austin computer. As seen in table 4, the calculation times for a fully 3D distribution using the Cray computer for irregularly shaped fields and heterogeneous anatomy was, in 1990, between three and four minutes for field sizes ranging from 50 mm to 200 mm on a side.

Fig. 33 Cray X-MP supercomputer located at the University of Texas - Austin campus, circa 1988.

Table 4 Calculation times for 3D dose calculations using three source model. Reproduced from Moyers [12].

Estimated Times in Seconds for Various Calculations on Cray X-MP/24

Type of Calculation	GENFAN	PNSHET	GENPEN	CONVOL (twice)	AD2ARA (twice)	Component Total	Beam Total
64x32x128 rectangular rectangular 1 cpu	0	1.6* 15.4*	0	2.6*	0.06*	4.3* 18.1	12.9* 54.3*
64x32x128 irregular rectangular 1 cpu	0	2.6 16.4	4	2.6*	0.06*	9.3 23.1	27.8 69.2
128x64x32 irregular fan 1 cpu	4	0.9 2.6	4	1.0	0.04	10.0 11.7	29.9 35.0
256x128x64 irregular fan 1 cpu	32	7.2 20.8	64	16.0	0.5	119.7 133.3	359.1 399.9
256x128x64 irregular fan 2 cpu	18	4.0 11.6	36	8.9	0.3	67.2 74.8	201.6 224.4

Note: top numbers for 5 cm by 5 cm field, bottom numbers for 20 cm by 20 cm field.

* = actual times based upon CPU time charges on one processor

VI. Summary

Sources of neutrons for FNT have included fission, fusion, stripping or breakup of light ions, or inelastic reactions. Fission sources have a high relative biological effect (RBE), a low oxygen enhancement ratio (OER), are very low penetrating, and pose a security risk in a public hospital. Fusion sources had small gantries, required only small treatment rooms, had low beam penetrations, had low dose rates, and required frequent tube changes. High energy beams made by protons or deuterons on beryllium targets have a high dose rate, are highly penetrating, but may undesirably have increased OER values.

Between 1970 and 1995 FNT facilities evolved from parasitic facilities to dedicated medical facilities; from low-energy (< 16 MeV) to high-energy (40 - 66 MeV) beams; from stationary gantries to fully rotating gantries; and from manually exchangeable rectangular collimators to automated MLCs. These advances served to reduce side-effects for treated patients but by the time these advances were realized, a sour taste for FNT had already been acquired by many radiation therapy practitioners. Near the end of this period, many people were discussing the possibilities of carbon ion treatments that could presumably offer the high-LET advantage of neutrons but the physical precision of protons. By the late 1990s, most FNT facilities around the world had shut down with only a few facilities further advancing the technology and continuing to treat patients. FNT could, however, serve as a lower-cost alternative to carbon ion treatments in some situations.

Acknowledgements

The author would like to express appreciation to Dr. Larry Beach, Dr. John Horton, and Dr. James Smathers for their guidance and support in the field of neutron therapy.

Unless otherwise specified, all photographs were taken by the author.

References

1. Stone, R. S. Larkin, J. C. (1942) "The treatment of cancer with fast neutrons" *Radiol.* 39: 608 - 620.
2. Catterall, M. Rogers, C. Thomlinson, R. H. Field, S. B. (1971) "An investigation into the clinical effects of fast neutrons. Methods and early observations" *Br. J. Radiol*. 44: 603 - 611. doi: 10.1259/0007-1285-44-524-603
3. Koester, L. Breit, A. Burger, G. (1981) "The Munich Therapy Project RENT" in *Treatment planning for external beam therapy with neutrons.* ed. Burger, G. Breit, A. Broese, J. J. (Urban & Schwarzenberg, Baltimore)
4. Specht, H. M. Neff, T. Reuschel, W. Wagner, F. M. Kampfer, S. Wilkens, J. J. Petry, W. Combs, S. E. (2015) "Paving the road for modern particle therapy - what can we learn from the experience gained with fast neutron therapy in Munich" *Frontiers in Oncology* 5: 262(1-5).
5. International Commission of Radiation Units and Measures (1989) "Clinical neutron dosimetry part 1: determination of absorbed dose in a patient treated by external beams of fast neutrons" *ICRU Report 45*.
6. Bloch, P. Larsen, R. Chu, J. (1983) "The neutron therapy facility at the University of Pennsylvania - Fox Chase Cancer Center" *IEEE Trans. Nucl. Sci.* 30(2): 1788 - 1792.
7. McFarlin, W. A. Suttle, A. D. (1971) "Fast neutron cancer therapy with the TAMVEC" *IEEE Transactions on Nuclear* 18(3): 780 - 781.
8. Almond, P. R. Smathers, J. B. Oliver, G. D. Hranitzky, E. B. Routt (1973) "Dosimetric properties of neutron beams produced by 16 - 60 MeV deuterons on beryllium" *Radiat. Res.* 54(1): 24 - 34.
9. Smith, A. R. Almond, P. R. Smathers, J. B. Otte, V. A. (1974) "Dosimetric Properties of the Fast Neutron Therapy Beams at TAMVEC" *Radiology* 113(1): 187 - 193. doi: 10.1148/113.1.187
10. Zink, S. Antoine, J. Mahoney, F. J. (1989) "Fast neutron therapy clinical trials in the United States: *Am. J. Clin. Oncol.* 12(4): 277 - 282.
11. Hendry, G. O. Hilton, J. L. Tom, J. L. (1977) "Neutron source development at the cyclotron corporation" *Int. J. Rad. Oncol. Bio. Phys.* 3: 367 - 372.
12. Moyers, M. F. (1991) *A convolution model for energy transport in a therapeutic fast neutron beam.* (University of Texas Graduate School of Biomedical Sciences at Houston) https://digitalcommons.library.tmc.edu/dissertations/AAI9202791
13. Almond, P. R. Zermeno, A. Marbach, J. R. Otte, V. Stafford, P. M. (1985) "The University of Texas M.D. Anderson Hospital Cyclotron Facility" in *Proceedings of the Fifth Symposium on Neutron Dosimetry* ed. Schraube, H. Burger, G. Booz, J. (Commission of the European Communities, Luxembourg) p. 979 - 987.
14. Horton, J. L. Otte, V. A. Schultheiss, T. E. Stafford, P. M. Sun, T. Zermeno, A. (1988) "Physical characteristics of the M. D. Anderson Hospital clinical neutron beam" *Radiother. Oncol.* 13(1): 17 - 22. doi: 10.1016/0167-8140(88)90293-9.
15. Zermeno, A. Cowart, R. Otte, V. et al. (1987) "Modification of a CP-42 Cyclotron to meet clinical needs" *Nuclear Instruments and Methods in Physics Research*. B24/25: 1100 - 1105.
16. Carroll, L. R. Ramsey, F. Armbruster, J. Montenero, M. (2001) "Recycling and recommissioning a used biomedical cyclotron" *Sixteenth International Conference on Applications of Accelerators in Research and Industry* eds. Duggan, J. L. Morgan, I. L. (American Institute of Physics) pp. 639 - 642.
17. Caderao, J. B. Hussey, D. H. Fletcher, G. H. Sampiere, V. A. Johnson, D. E. Wharton, J. G. (1976) "Fast neutron radiotherapy for locally advanced pelvic cancer" *Cancer* 37: 2620 - 2629.
18. Moyers, M. F. Lesyna, W. (2004) "Isocenter characteristics of an external ring proton gantry" *Int. J. Radiation, Oncology, Biology, Physics* 90(5): 1622 - 1630.
19. Blosser, H. DeKamp, J. Johnson, D. Marti, F. Milton, B. Vincent, J. Blosser, G. Jemison, E. Maughan, R. Powers, W. Purcell, J. Young, W. (1985) "Compact superconducting cyclotrons for neutron therapy" *IEEE Transactions on Nuclear Science* NS-32(5): 3287 - 3291.
20. Maughan, R. L. Blosser, G. F. Blosser, E. B. Blossser, H. G. Powers, W. E. (1989) "Transmission measurements in multi-rod arrays: a design study for a multi-rod collimator" *Radiotherapy and Oncology* 15: 125 - 131.
21. Wambersie, A. Richard, F. Breteau, N. (1994) "Development of fast neutron therapy worldwide - Radiobiological, clinical and technical aspects" *Acta Oncol.* 33(3): 261 - 274.
22. Moyers, M. F. Horton, J. L. Boyer, A. L. (1988) "A scatter model for fast neutron beams using convolution of diffusion kernels" *Radiation Protection Dosimetry* 23: 475 - 478. doi: 10.1093/oxfordjournals.rpd.a080224
23. Moyers, M. F. (1992) "Neutron beam energy transport calculations by combining Monte Carlo and convolution techniques" *New Horizons in Radiation Protection and Shielding* (Illinois: American Nuclear Society, Inc.) p. 80 - 85.
24. Moyers, M. F. Horton, J. L. (1990) "Determination of the neutron and photon spectra of a clinical fast neutron beam" *Medical Physics* 17(4): 607 - 614.

Contacts of the corresponding author:

Author: Michael Farley Moyers
Institute: Shanghai Proton and Heavy Ion Center
Street: 4365 Kangxin Road
City: Shanghai
Country: China
Email: Michael.F.Moyers@sphic.org.cn